Electromagnetic Scattering by the Multielements Periodic Grating of Circular Cylinders and the Dielectric Slab

Jandieri, Vakhtang
Department of Computer Science and Communication Engineering, Graduate School of Information Science and Electrical Engineering, Kyushu University : Graduate Student

Yasumoto, Kiyotoshi
Department of Computer Science and Communication Engineering, Faculty of Information Science and Electrical Engineering, Kyushu University

https://doi.org/10.15017/1516053

出版情報：九州大学大学院システム情報科学紀要. 10 (1), pp.1-7, 2005-03-25. 九州大学大学院システム情報科学研究院
バージョン：
権利関係：

九州大学大学院
システム情報科学紀要
第10巻 第1号 平成17年3月

Research Reports on Information Science and
Electrical Engineering of Kyushu University
Vol.10, No.1, March 2005

Electromagnetic Scattering by the Multielements Periodic Grating of Circular Cylinders and the Dielectric Slab

Vakhtang JANDIERI* and Kiyotoshi YASUMOTO**

Abstract: An accurate formulation to the problem of electromagnetic scattering by the multielements periodic grating of circular cylinders and dielectric slab is presented. The dielectric cylinders are assumed to have different radii and geometrical locations per unit cell and the dielectric slab is located apart from the periodic grating. Applying the boundary conditions and using the additional theorem for the cylindrical functions and the projection method, an infinite system of linear equations for the unknown coefficients of the multipole spectra is obtained. This system of equations is solved by the reduction method and the analytical expressions for both transmission and reflection coefficients are derived by using the relationship between the diffracted spectra and the multipole spectra. The numerical examples demonstrate the multiple scattering effects between the cylindrical elements of the grating and the slab boundaries on the frequency response in the transmission coefficient. It is shown that the frequency response could be controllable by properly adjusting the geometrical parameters of the dielectric slab.

Keywords: Transmission coefficient, Multielements grating, Dielectric slab, Multipole spectrum, Reduction method

1. Introduction

Scattering of electromagnetic waves by artificial inhomogeneities such as periodic gratings of cylindrical objects plays an important role in antenna technology, radiophysics and optics. Very recently, dielectric or metallic structures[1] are under a growing attention for their promising applications to frequency selective or polarization selective devices in microwaves and optical waves, narrow-band filters, modern communication problems for improvement radio-electronic and communication systems. Therefore, various analytical or numerical techniques[2)-9)] have been developed to formulate the electromagnetic wave scattering from the periodic structures.

The purpose of this paper is to present an accurate formulation for the two-dimensional diffraction of electromagnetic waves by the multielements periodic grating of the circular dielectric cylinders and the dielectric slab, when it is located apart from the grating. Cylinders are assumed to have different radii and geometrical locations per unit cell. Such a periodic structure is very attractive to devise a novel wavelength and polarization selective components in microwave and optical wave regions, because additional degrees of freedom for controlling the scattered fields are available. In the formulation, firstly, the scattered fields are written in terms of the expansion into multipole and diffracted spectra. Applying the boundary conditions on the surface of the dielectric slab, amplitudes of the transmitted and reflected waves from the slab are expressed through the amplitudes of the diffracted space harmonic fields from the periodic grating of the circular cylinders. Then the addition theorem for the cylindrical functions and the projection method are used to obtain an infinite system of linear equations for the unknown coefficients of the multipole spectra. The system of equations is solved using the reduction method. Finally, the amplitude of the diffracted space harmonic fields from the periodic grating of circular cylinders is calculated using the coefficient of the multipole spectra of cylindrical waves. The convergence and stability of the solutions are numerically tested by analyzing the dependence of the transmission coefficient on the truncation order of the scattered fields. Numerical examples for the transmission coefficient of the fundamental space harmonic are presented for the dielectric slab and the periodic grating with up to two circular dielectric cylinders per unit cell. Transmission characteristics are substantially influenced by the presence of the dielectric slab and various interesting features of the frequency response are demonstrated, which are not attainable for the multielement

* Department of Computer Science and Communication Engineering, Graduate Student
** Department of Computer Science and Communication Engineering

periodic grating without the dielectric slab.[12),13)] It is shown that the location of the resonance peaks could be controllable by adjusting the distance between the dielectric slab and the periodic grating and the thickness of the slab. The time dependence of the fields is assumed to be $\exp(i\omega t)$ and omitted throughout the paper.

2. Formulation of the problem

The geometry of the problem is illustrated in the **Fig. 1**.

A periodic array of N-parallel circular cylinders per unit cell is located in free space with permittivity ϵ_0 and permeability μ_0. The structure is uniform in the z-direction and periodic in the y-direction with a period d. N cylinders within the unit cell are assumed to have different radii and material constants. The integers ν and μ are used to denote the number of the cells and the number of the cylinders located within the cell, $\ell_{\mu\mu'}$ is the distance between two centers of the μ-th and μ'-th cylinders located in the unit cell. The dielectric slab with a thickness η, permittivity ϵ and permeability μ is located at a distance h from the periodic grating. Assume that E-polarized plane wave with unit amplitude is incident on this grating from the upper region with an angle θ relative to the positive x-axis. Then the incident wave is given as:

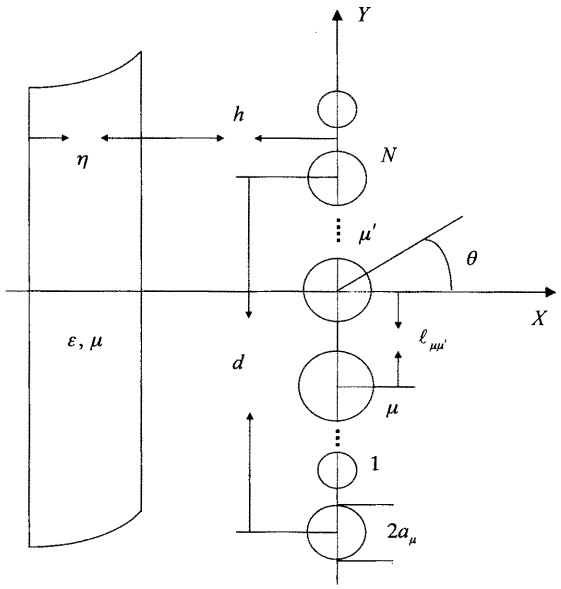

Fig. 1 Cross section of N-element periodic arrays of cylindrical objects and dielectric slab.

$$E_{zinc}=\exp[ik(x\cos\theta+y\sin\theta)],\quad k=\omega\sqrt{\epsilon_0\mu_0}. \tag{1}$$

The scattered fields are expressed in terms of the expansion into multipole and diffracted spectra in different regions as follows:

$$E_{zsc}=\sum_{\nu=-\infty}^{\infty}\sum_{m=-\infty}^{\infty}\sum_{\mu=1}^{N}X_m^{(\mu)}H_m^{(2)}(kr_{\nu\mu})\exp[ik(\nu d+\ell_{\mu 1})\sin\theta + im\varphi_{\nu\mu}],\ (r_{\nu\mu}\geq a_\mu) \tag{2}$$

$$E_{zi}^{(\nu,\mu)}=\sum_{m=-\infty}^{\infty}Y_m^{(\mu)}J_m(k_\mu r_{\nu\mu})\exp[ik(\nu d+\ell_{\mu 1})\sin\theta + im\varphi_{\nu\mu}],\ (0\leq r_{\nu\mu}\leq a_\mu) \tag{3}$$

$$E_{z1}=E_{zinc}+E_{zsc}+\sum_{p=-\infty}^{\infty}F_p\exp(ig_py-ih_px),\quad x\geq -h \tag{4}$$

$$E_{z2}=\sum_{p=-\infty}^{\infty}\{C_p\exp[ih'_p(x+h)] + D_p\exp[-ih'_p(x+h)]\}\exp(ig_py),\quad (-h-\eta\leq x\leq -h) \tag{5}$$

$$E_{z3}=\sum_{p=-\infty}^{\infty}T_p\exp[ig_py+ih_p(x+h+\eta)],\quad (x\leq -h-\eta) \tag{6}$$

$$E_{zsc}=\begin{cases}\sum_{p=-\infty}^{\infty}A_p^{+}\exp(ig_py+ih_px), & -h\leq x\leq -a_\mu\\ \sum_{p=-\infty}^{\infty}A_p^{-}\exp(ig_py-ih_px), & x\geq a_\mu\end{cases} \tag{7}$$

where a_μ is a radius of the μ-th cylinder, $k_\mu=\omega\sqrt{\epsilon_\mu\mu_\mu}$ and $k'=\omega\sqrt{\epsilon\mu}$ are the wave-numbers of the μ-th cylinder and the dielectric slab, respectively. $H_m^{(2)}$ is the m-th order Hankel function of the second kind and J_m is Bessel function of the m-th order, $X_m^{(\mu)}$ and $Y_m^{(\mu)}$ are the unknown coefficients of the multipole spectra, $g_p=\frac{2\pi p}{d}+k\sin\theta$, $h_p=(k^2-g_p^2)^{1/2}$ and $h'_p=(k'^2-g_p^2)^{1/2}$, $A_p^{\pm}$ are the amplitudes of the p-th order transmitted and reflected waves from the periodic grating of the circular cylinders. C_p and D_p are the amplitudes of transmitted and reflected waves inside the slab. T_p and F_p are the amplitudes of the p-th order transmitted and reflected waves from the dielectric slab, respectively. The scattered fields must satisfy the following boundary conditions:

$$E_{z1}=E_{z2},\ \frac{1}{i\omega\mu_0}\frac{\partial}{\partial x}E_{z1}=\frac{1}{i\omega\mu}\frac{\partial}{\partial x}E_{z2};\ \text{at } x=-h \tag{8}$$

$$E_{z2}=E_{z3},\ \frac{1}{i\omega\mu}\frac{\partial}{\partial x}E_{z2}=\frac{1}{i\omega\mu_0}\frac{\partial}{\partial x}E_{z3};\ \text{at } x=-h-\eta \tag{9}$$

$$E_{z1}=E_{zi}^{(\nu,\mu)},\ \frac{1}{i\omega\mu_0}\frac{\partial}{\partial r_{\nu\mu}}E_{z1}=\frac{1}{i\omega\mu_\mu}\frac{\partial}{\partial r_{\nu\mu}}E_{zi}^{(\nu,\mu)};\quad \text{at } r_{\nu\mu}=a_\mu,\ 0\leq\varphi_{\nu\mu}\leq 2\pi \tag{10}$$

Substituting (4)-(7) into the boundary conditions (8)

and (9) on the surface of the dielectric slab, the unknown coefficients F_p, B_p, C_p and D_p could be easily expressed in terms of $A_p^{\pm}$ as follows:

$$\begin{aligned}
F_p&=(A_p^{\pm}+\delta_{p0})r_p\\
T_p&=(A_p^{\pm}+\delta_{p0})\eta_p\\
C_p&=(1/2)(A_p^{\pm}+\delta_{p0})[(1+a_1)\exp(-ia_2)\\
&\quad+r_p(1-a_1)\exp(ia_2)]\\
D_p&=(1/2)(A_p^{\pm}+\delta_{p0})[(1-a_1)\exp(-ia_2)\\
&\quad+r_p(1+a_1)\exp(ia_2)]
\end{aligned}\tag{11}$$

where

$$\begin{aligned}
r_p&=-\frac{(1-a_1^2)\exp(-2ia_2)\sin a_3}{(1+a_1^2)\sin a_3-2ia_1\cos a_3}\\
\eta_p&=\frac{\exp(-ia_2)}{\cos a_3+(i/2)[(1/a_1)+a_1]\sin a_3}\\
a_1&=h_p\mu/h'_p\mu_0,\quad a_2=h_ph,\quad a_3=h'_p\eta
\end{aligned}\tag{12}$$

When the boundary conditions (10) are fulfilled on the surface of the μ-th cylinder of the zero-th cell ($\nu=0$), using the addition theorem for cylindrical functions[10], projection method and the expression for the amplitude of the diffracted p-th order space harmonic given by (see Appendix)

$$\begin{aligned}
A_p^{\pm}=&\frac{1}{\pi\sqrt{D^2-(p+D\sin\theta)^2}}\sum_{m=-\infty}^{\infty}\sum_{\mu=1}^{N}X_m^{(\mu)}i^{\mp m}\\
&\exp(\pm im\varphi_p)\exp\left(-i\frac{2\pi p}{d}\ell_{\mu 1}\right),
\end{aligned}\tag{13}$$

the infinite system of linear equations with respect to the unknown coefficient $X_n^{(\mu)}$ is derived as follows[12),13)]:

$$X_n^{(\mu)}=a_n^{(\mu)}+\sum_{j=1}^{N}\sum_{m=-\infty}^{\infty}X_m^{(j)}Q_{nm}^{(j)}\tag{14}$$

where

$$\begin{aligned}
a_n^{(\mu)}&=-[i^n\exp(-in\theta)+i^{-n}r_0\exp(in\ tg\theta)]\zeta_n^{(\mu)}\\
Q_{nm}&=-(1-\delta_{nm}\delta_{\mu j})[L_{m-n}(kd,\ k\ell_{\mu j},\ \theta)\\
&\quad+\Delta_{n+m}(\chi_{\mu j})]\zeta_n^{(\mu)}
\end{aligned}\tag{15}$$

$$\begin{aligned}
\zeta_n^{(\mu)}=&J_n(a_\mu)\{H_n^{(2)}(a_\mu)+J_n(a_\mu)[L_0(kd,\ 0,\ \theta)\\
&+\Delta_{2n}(0)]-\eta_n^{(\mu)}(a_\mu,\ \tilde{a}_\mu)J_n(\tilde{a}_\mu)\}^{-1}
\end{aligned}\tag{16}$$

$$\eta_n^{(\mu)}(a_\mu,\ \tilde{a}_\mu)=\frac{2i}{\pi a_\mu}\left[J'_n(a_\mu)J_n(\tilde{a}_\mu)-\frac{Z_0}{Z_\mu}J_n(a_\mu)J'_n(\tilde{a}_\mu)\right]^{-1}\tag{17}$$

$$\begin{aligned}
&\Delta_{n+m}(\chi_{\mu j})\\
&=i^{-n-m}\sum_{p=D(1+\sin\theta)}^{D(1-\sin\theta)}\frac{r_p\exp[i(n+m)\varphi_p]\exp(ip\chi_{\mu j})}{\pi\sqrt{D^2-(p+D\sin\theta)^2}},
\end{aligned}\tag{18}$$

$$a_\mu=ka_\mu,\ \tilde{a}_\mu=k_\mu a_\mu,\ Z_\mu=\sqrt{\frac{\mu_\mu}{\epsilon_\mu}},\ \chi_{\mu j}=k\ell_{\mu j}\mathrm{sgn}(\mu-j)/D\tag{19}$$

$\varphi_p=arctg\dfrac{p+D\sin\theta}{\sqrt{D^2-(p+D\sin\theta)^2}}$, $D=d/\lambda$. L_{m-n} is the $(m-n)$-th order Lattice Sums, which is expressed by a semi-infinite series of Hankel functions. To overcome the difficulty of a very slow convergence of the series, we use an integral form[5)] of the lattice sums, which can be accurately and efficiently evaluated using a simple scheme of numerical integration. Since the terms a_n and Q_{nm} satisfy a condition of square-law convergence on the module as:

$$\sum_n|a_n|^2<\infty,\quad \sum_{n,m}|Q_{nm}|^2<\infty\tag{20}$$

(14) could be solved by using the reduction method[11)]. The solution $X_n^{(\mu)}$ obtained for a truncated system of linear equations tends to the exact one with increasing the truncation order of the system. The convergence and stability of the solutions to (14) could be validated by numerically testing the dependence of the transmission coefficient $|T_0|=|(1+A_0^+)\eta_0|$ and reflection coefficient $|R_0|=|F_0+A_0^-|$ of the main space harmonic on the truncation order of the system. The case of the H-polarized wave can be treated in the same manner by employing H_z field as the leading field and introducing the following substitutions into the results for E-polarized wave:

$$\begin{aligned}
&\epsilon_0\longrightarrow-\mu_0,\ \epsilon_\mu\longrightarrow-\mu_\mu,\\
&\mu_0\longrightarrow\epsilon_0,\ \mu_\mu\longrightarrow\epsilon_\mu,
\end{aligned}\tag{21}$$

3. Numerical Results

The proposed formulation has been used to analyze the transmission and reflection properties of multielements gratings of circular cylinders and dielectric slab. Although a substantial number of numerical examples could be generated, we discuss here the transmission characteristics of the dielectric slab and the periodic grating with up to two dielectric circular cylinders per unit cell for the frequency range $0\le d/\lambda\le 1.0$ under the normal incidence of plane wave, because such a situation is essential to the use of periodic arrays as the frequency and polarization selective components. The numerical examples in what follows were obtained with the errors in the energy conservation less than 10^{-5} by truncating the infinite system of linear Eq. (14) at $n=\pm 7$. The numerical examples in what follows have been calculated using the non-dimensional parameters: $s_1=2a_1/d$, $s_2=2a_2/d$, $\epsilon_{r1}=\epsilon_1/\epsilon_0$, $\epsilon_{r2}=\epsilon_2/\epsilon_0$, $\ell=\ell_{12}/d$, $\tilde{\epsilon}=\epsilon/\epsilon_0$,

$\tilde{h}=h/d$ and $\tilde{\eta}=\eta/d$.

The transmission coefficient T_0 of the fundamental space harmonic is shown in **Fig. 2** as function of normalized wavelength d/λ for the TM wave, where $\tilde{\eta}=0.2$, $\tilde{h}=0.4$, $\tilde{\epsilon}=2.0$, $s_1=0.6$ and $\epsilon_1=2.0$. For comparison, the transmission coefficient for the one-element grating with one dielectric circular cylinder per unit cell is also plotted by the dotted line.

The transmission characteristics are substantially changed due to the multiple scattering effects between the cylindrical elements of the periodic grating and the dielectric slab. There exists only one reflection peak for the one-element grating. When the dielectric slab is additionally placed apart from the periodic grating, the reflection peak splits into two peaks and a broad-band resonance profile is obtained. Perfect pass-band region can be also observed over a wide range of the wavelength $0.9\leq d/\lambda\leq 0.95$. In case of one-element grating the TM wave is completely reflected at $d/\lambda=0.923$, while at the presence of the dielectric slab it is completely transmitted at the same frequency. To discuss the effect of presence of the dielectric slab in more detail, we consider the influence of the distance between the dielectric slab and the periodic grating and the thickness of the slab on the frequency response in transmittance. Dependence of transmission coefficient T_0 of the fundamental space harmonic versus normalized wavelength d/λ for different thicknesses of the slab is shown in **Fig. 3**. For comparison, the transmission coefficient for the one-element grating is also plotted by the dotted line. It could be vividly seen that the resonance peaks are shifting to the long wavelength region and the pass-band is broadening with increasing the thickness of the dielectric slab. **Figure 4** illustrates how the transmission coefficient is influenced by changing the

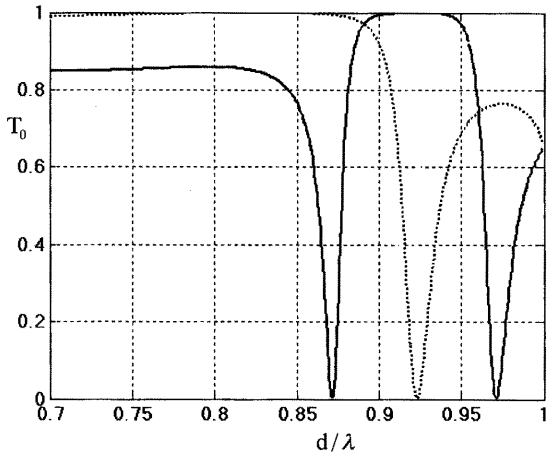

Fig. 2 One-element grating with dielectric slab: $\tilde{\eta}=0.2$, $\tilde{h}=0.4$, $\tilde{\epsilon}=2.0$, $s_1=0.6$, $\epsilon_1=2.0$, TM wave (solid); One-element grating: $\tilde{\eta}=0$, $s_1=0.6$, $\epsilon_1=2.0$, TM wave (dotted).

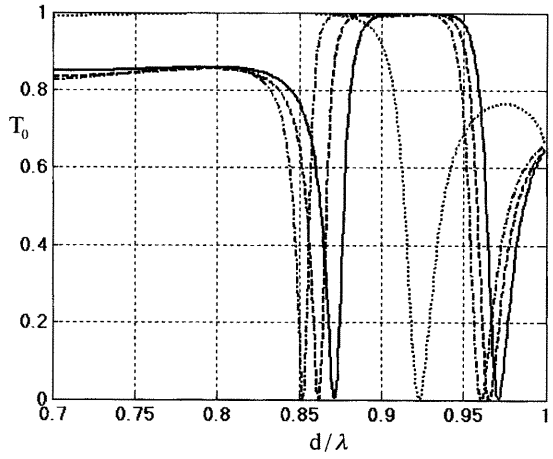

Fig. 3 One-element grating with dielectric slab: $\tilde{\eta}=0.2$, $\tilde{h}=0.4$, $\tilde{\epsilon}=2.0$, $s_1=0.6$, $\epsilon_1=2.0$, TM wave (solid); $\tilde{\eta}=0.25$, $\tilde{h}=0.4$, $\tilde{\epsilon}=2.0$, $s_1=0.6$, $\epsilon_1=2.0$, TM wave (dashed); $\tilde{\eta}=0.3$, $\tilde{h}=0.4$, $\tilde{\epsilon}=2.0$, $s_1=0.6$, $\epsilon_1=2.0$, TM wave (dot-dashed); One-element grating: $\tilde{\eta}=0$, $s_1=0.6$, $\epsilon_1=2.0$, TM wave (dotted).

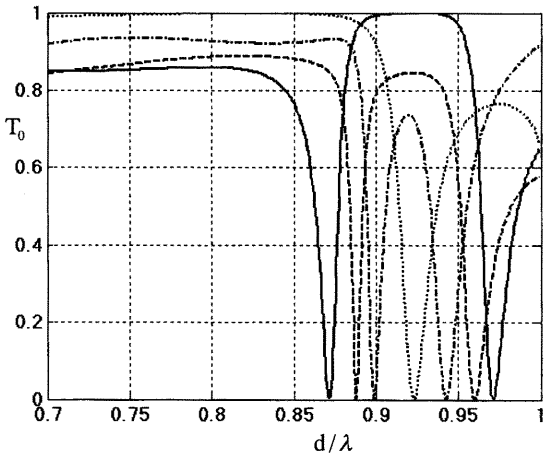

Fig. 4 One-element grating with dielectric slab: $\tilde{\eta}=0.2$, $\tilde{h}=0.4$, $\tilde{\epsilon}=2.0$, $s_1=0.6$, $\epsilon_1=2.0$, TM wave (solid); $\tilde{\eta}=0.2$, $\tilde{h}=0.55$, $\tilde{\epsilon}=2.0$, $s_1=0.6$, $\epsilon_1=2.0$, TM wave (dashed); $\tilde{\eta}=0.2$, $\tilde{h}=0.7$, $\tilde{\epsilon}=2.0$, $s_1=0.6$, $\epsilon_1=2.0$, TM wave (dot-dashed); One-element grating: $\tilde{\eta}=0$, $s_1=0.6$, $\epsilon_1=2.0$, TM wave (dotted).

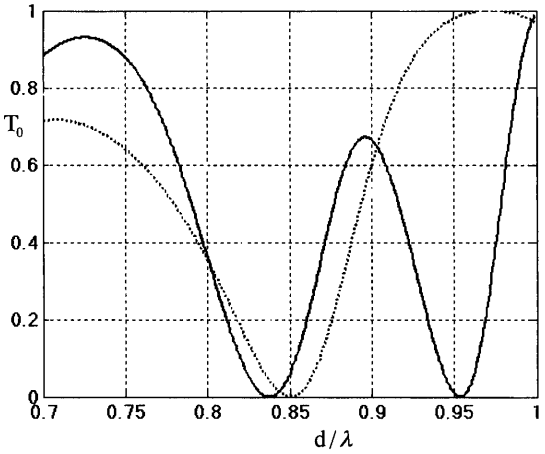

Fig. 5 Two-element grating with dielectric slab: $\tilde{\eta}=0.2$, $\tilde{h}=0.4$, $\tilde{\epsilon}=2.0$, $s_1=0.6$, $\epsilon_1=2.0$, $s_2=0.35$, $\epsilon_2=7.5$, TM wave (solid); Two-element grating: $\tilde{\eta}=0$, $s_1=0.6$, $\epsilon_1=2.0$, $s_2=0.35$, $\epsilon_2=7.5$, TM wave (dotted).

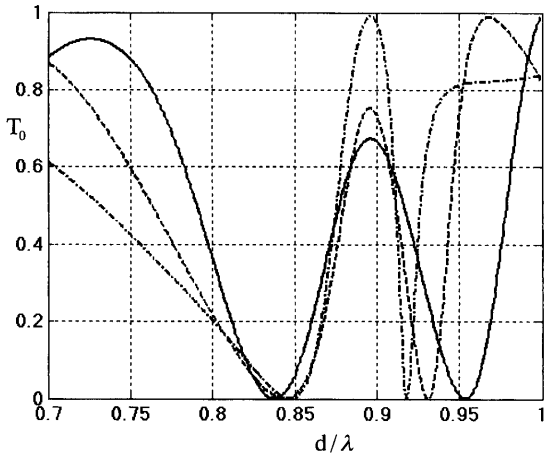

Fig. 6 Two-element grating with dielectric slab: $\tilde{\eta}=0.2$, $\tilde{h}=0.4$, $\tilde{\epsilon}=2.0$, $s_1=0.6$, $\epsilon_1=2.0$, $s_2=0.35$, $\epsilon_2=7.5$, TM wave (solid); $\tilde{\eta}=0.2$, $\tilde{h}=0.55$, $\tilde{\epsilon}=2.0$, $s_1=0.6$, $\epsilon_1=2.0$, $s_2=0.35$, $\epsilon_2=7.5$, TM wave (dashed); $\tilde{\eta}=0.2$, $\tilde{h}=0.7$, $\tilde{\epsilon}=2.0$, $s_1=0.6$, $\epsilon_1=2.0$, $s_2=0.35$, $\epsilon_2=7.5$, TM wave (dot-dashed).

distance between the dielectric slab and the periodic grating of the circular dielectric cylinders with other parameters same as those in **Fig. 2** and **Fig. 3**. It is shown that the separation distance between the two resonance peaks is gradually getting smaller and the narrow-band resonance profile is obtained increasing the distance between the slab and the periodic grating. It could be explained due to the multiple scattering effects between the slab and the cylindrical elements of the periodic grating. Consequently, from **Fig. 3** and **Fig. 4** it follows that the location of the resonance peaks could be controllable the properly adjusting the geometrical parameters of the dielectric slab.

The multielement periodic grating introduces additional degrees of freedom to realize a variety of wavelength in transmission and reflection. Eight independent parameters s_1, s_2, ϵ_1, ϵ_2, ϵ, ℓ, h and η are available to adjust the transmission and reflection characteristics. As an example, the transmission coefficient T_0 of the fundamental space harmonic as function of normalized wavelength d/λ for the TM wave is shown in **Fig. 5** and **Fig. 6**. Symmetrical configuration of the grating has been considered, where the cylinders per unit cell are placed with an equal distance from each other $\ell=0.5$. **Figure 5** vividly illustrates that in comparison to the two-element grating with two dielectric cylinders per unit cell, the presence of the dielectric slab apart from the grating leads to the appearance of two resonance peaks with quite a broad bandwidth at $d/\lambda=0.838$ and $d/\lambda=0.954$, respectively.

The resonance peaks become to be well separated and a broad-band resonance profile is obtained. From **Fig. 6** it follows that the frequency response in transmittance is strongly influenced by the location of the dielectric slab with respect to the periodic grating. Resonance wavelengths and their relative separation could be controlled by adjusting the distance between the periodic grating of dielectric circular cylinders and the dielectric slab.

4. Conclusion

An accurate formulation for the two-dimensional diffraction of electromagnetic plane waves by multielements periodic grating of dielectric circular cylinders and the dielectric slab has been proposed. The cylinders have been assumed to have different radii and geometrical location per unit cell. Applying the boundary conditions, the addition theorem for the cylindrical functions and the projection method, an infinite system of linear equations to determine the unknown coefficients of the multipole spectrum was derived. The linear equations were solved by the reduction method and the convergence and stability of the numerical solutions were tested for various

parameters of the grating. Numerical examples of the transmission coefficient were presented for the dielectric slab and the periodic grating with up to two dielectric circular cylinders per unit cell. Various interesting features of the frequency response in transmittance were demonstrated, which are not attainable for the periodic grating without the dielectric slab. The frequency response is significantly affected by the multiple scattering between the dielectric slab and the cylindrical elements of the periodic grating and could be controllable by adjusting the geometrical parameters of the dielectric slab.

References

1) A. Scherer, T. Doll, E. Yablonovitch, H.O. Everitt, and J.A. Higgins: "Special Section on Electromagnetic Crystal Structures, Design, Synthesis, and Applications," J. Lightwave Technol., Vol.17, no.11, pp.1928-2207 (1999).
2) V. Twersky: "On Scattering of Waves by the Infinite Grating of Circular Cylinders," IRE Trans. Antennas Propagat, Vol.10 (1962).
3) R. Petit: Electromagnetic Theory of Gratings, Springer-Verlag, Berlin (1980).
4) W.C. Chew: Waves and Fields in Inhomogeneous Media, Van Nostrand Reinhold, New York (1990).
5) K. Yasumoto and K. Yoshitomi: "Efficient Calculation of Lattice Sums for Free-Space Periodic Green's Function", IEEE Transactions on Antennas and Propagation, Vol.47, no.6, pp.1050-1055 (June, 1999).
6) K.Yasumoto and H. Jia: "Three-Dimensional electromagnetic scattering from multilayered periodic arrays of circular cylinders," Proceedings of 2002 China-Japan Joint Meeting on Microwaves, pp.301-304 (2002).
7) T. Kushta and K. Yasumoto: "Electromagnetic Scattering from Periodic Arrays of Two Circular Cylinders per Unit Cell," Progress in Electromagnetics Research, PIER 29, pp.69-85 (2000).
8) F.G. Bogdanov, G.Sh. Kevanishvili: Diffraction gratings and waveguide discontinuities. -Monograph. - Samshoblo, Tbilisi (1994), (in Russian).
9) G. Pelosi, A. Cocchi and A. Monorchio: "A Hybrid FEM-based procedure for the scattering from photonic crystals illuminated by a Gaussian beam," IEEE Trans., Antennas Propagat., Vol.48, pp.973-980 (2000).
10) M. Abramowitz and Irene A. Stegun: Handbook of Mathematical Functions (1964).
11) L.V. Kantorovich and G.P. Akilov: Functional Analysis, Pergamon Press, New-York (1982).
12) V. Jandieri and K. Yasumoto: "Diffraction of plane waves by multielements grating of the circular cylinders," IEEJ Transaction on fundamentals and Materials, Vol.124, no.12, pp.1148-1153 (December, 2004).
13) V. Jandieri and K. Yasumoto: "Diffraction of Plane Waves by Multielement Grating," URSI 2004 International Symposium on Electromagnetic Theory, Vol.2, pp.999-1001 (May, 2004).

Appendix

Using the Floquet theorem, the field scattered from the multielements periodic grating may be expressed in terms of a series of the multipole spectra based on the cylindrical waves or a series of the space harmonic waves as follows:

$$E_{z1}=\sum_{m=-\infty}^{\infty}\sum_{\nu=-\infty}^{\infty}\sum_{\mu=1}^{N}X_m^{(\mu)}H_m^{(2)}(kr_{\nu\mu})\exp[ik(\nu d+\ell_{\mu 1})\sin\theta+im\varphi_{\nu\mu}],\quad (r_{\nu\mu}\geq a_\mu) \tag{A. 1}$$

$$E_{z1}=\begin{cases}\sum_{p=-\infty}^{\infty}A_p^{+}\exp(ig_py+ih_px), & (x\leq -a_\mu)\\ \sum_{p=-\infty}^{\infty}A_p^{-}\exp(ig_py-ih_px), & (x\geq a_\mu)\end{cases} \tag{A. 2}$$

where

$$g_p=\frac{2\pi p}{d}+k\sin\theta,\quad h_p=\sqrt{k^2-g_p^2}. \tag{A. 3}$$

Defining the space harmonic waves propagating in the opposite direction with respect to the y axis by:

$$E_p^{+}=\exp(-ig_py+ih_px),\quad E_p^{-}=\exp(-ig_py-ih_px), \tag{A. 4}$$

the following relation is derived:

$$E_p^{\pm}\Delta E_{z1}-E_{z1}\Delta E_p^{\pm}=0 \tag{A. 5}$$

where Δ is the two-dimensional Laplace's operator. Applying the Green's theorem to Eq. (A. 5), we obtain:

$$\oint_{\Gamma}\left(E_p^{\pm}\frac{\partial E_{z1}}{\partial n}-E_{z1}\frac{\partial E_p^{\pm}}{\partial n}\right)d\Gamma =-\sum_{\mu=1}^{N}\oint_{\ell_\mu}\left(E_p^{\pm}\frac{\partial E_{z1}}{\partial n}-E_{z1}\frac{\partial E_p^{\pm}}{\partial n}\right)d\ell \tag{A. 6}$$

where $\tilde{\ell}_\mu$ ($\mu=1, 2.....N$) and Γ are circular and rectangular contours of the radii a_μ and the unit cell respectively; n denotes the coordinate normal to the contours. The calculation of the integral over the contour Γ yields:

$$A_p^{\pm}=\frac{1}{2ih_pd}\sum_{\mu=1}^{N}\oint_{\ell_\mu}\left(E_p^{\mp}\frac{\partial E_{z1}}{\partial n}-E_{z1}\frac{\partial E_p^{\mp}}{\partial n}\right)d\ell. \tag{A. 7}$$

On the other hand, expression of the scattered field E_{z1} for the μ-th cylinder of the zero-th cell ($\nu=0$) could be written in the form:

$$E_{z1}^{(\mu)}=\sum_{m=-\infty}^{\infty}[X_m^{(\mu)}H_m^{(2)}(kr_\mu)+Q_m(kd,\ \theta)J_m(kr_\mu)]\times \exp(ik\ell_{\mu 1}\sin\theta+im\varphi_\mu) \quad \text{(A. 8)}$$

where

$$Q_m(kd,\ \theta)=\sum_{q=-\infty}^{\infty}\left[X_q^{(\mu)}L_{q-m}^{(\mu)}(kd,\ 0,\ \theta)+\sum_{\substack{j=1\\ j\neq\mu}}^{N}X_q^{(j)}L_{q-m}^{(j)}(kd,\ k\ell_{\mu j},\ \theta)\right]. \quad \text{(A. 9)}$$

Substituting Eqs. (A. 4) and (A. 8) into Eq. (A. 7) and taking into account the expression of Wronskians for the cylindrical functions:

$$J_n'(\alpha_\mu)H_n^{(2)}(\alpha_\mu)-J_n(\alpha_\mu)H_n'^{(2)}(\alpha_\mu)=\frac{2i}{\pi\alpha_\mu}, \quad \text{(A. 10)}$$

the relationship (13) between the unknown coefficient of the multipole spectrum and the amplitude of the diffracted p-th order space harmonic is obtained.